Theor Appl Climatol
DOI 10.1007/s00704-013-0872-6

ORIGINAL PAPER

Mechanism on how the spring Arctic sea ice impacts the East Asian summer monsoon

Dong Guo · Yongqi Gao · Ingo Bethke · Daoyi Gong · Ola M. Johannessen · Huijun Wang

Received: 20 September 2012 / Accepted: 26 February 2013

Abstract Observational analysis and purposely designed coupled atmosphere–ocean (AOGCM) and atmosphere-only (AGCM) model simulations are used together to investigate a new mechanism describing how spring Arctic sea ice impacts the East Asian summer monsoon (EASM). Consistent with previous studies, analysis of observational data from 1979 to 2009 show that spring Arctic sea ice is significantly linked to the EASM on inter-annual timescales. Results of a multivariate Empirical Orthogonal Function analysis reveal that sea surface temperature (SST) changes in the North Pacific play a mediating role for the inter-seasonal connection between spring Arctic sea ice and the EASM. Large-scale atmospheric circulation and precipitation changes are consistent with the SST changes. The mechanism found in the observational data is confirmed by the numerical experiments and can be described as follows: spring Arctic sea ice anomalies cause atmospheric circulation anomalies, which, in turn, cause SST anomalies in the North Pacific. The SST anomalies can persist into summer and then impact the summer monsoon circulation and precipitation over East Asia. The mediating role of SST changes is highlighted by the result that only the AOGCM, but not the AGCM, reproduces the observed sea ice-EASM linkage.

D. Guo · Y. Gao · H. Wang
Nansen-Zhu International Research Center,
Institute of Atmospheric Physics, Chinese Academy of Sciences, Beijing 100029, China

Y. Gao (✉) · O. M. Johannessen
Nansen Environmental and Remote Sensing Center,
Thormøhlens gate 47, 5006 Bergen, Norway
e-mail: gyq@mail.iap.ac.cn

I. Bethke
Bjerknes Center for Climate Research,
Bergen, Norway

D. Gong
State Key Laboratory of Earth Surface Processes and Resource Ecology, Beijing Normal University,
Beijing 100875, China

1 Introduction

Global warming is enhanced at high latitudes where Arctic surface air temperature has risen twice as much as the global average in recent decades—a feature called Arctic amplification (e.g., Bekryaev et al. 2010). Data-based analyses indicate that the recent Arctic warming signal is broadly consistent with the reduction in sea ice cover (Screen and Simmonds 2010). Although the Arctic warming implies a melting sea ice cover (e.g., Johannessen et al. 2004; Johannessen 2008), its dynamic-thermodynamic response is neither straightforward nor necessarily linear (Zhang et al. 2000) nor is the response of the atmosphere to sea ice reductions (Magnusdottir et al. 2004; Deser et al. 2004).

Numerous observational and model-based studies also suggest that Arctic sea ice changes in turn impact regional and remote climate (for a review, refer to Budikova 2009). For instance, using an atmosphere general circulation model (AGCM) Mesquita et al. (2010) found that winter sea ice cover over the Sea of Okhotsk may affect most storm track variables in the North Pacific. Fan (2007) found from a statistical analysis that sea ice cover over North Pacific could be a potential predictor for the typhoon frequency over west North Pacific. Through an analysis of observed data and AGCM modeling experiments, Zhao et al. (2004) noted the close relationship between the spring sea ice cover in the Bering Sea and the Sea of Okhotsk and rainfall variability in the East Asian summer monsoon (EASM). By analysing observational and reanalysis data from the last 30 years, Wu et al. (2009a) found a significant correlation between the spring Arctic sea ice concentration (ASIC) and

Published online: 23 March 2013

summer rainfall over China. Honda et al. (1996, 1999) investigated the atmospheric response to winter sea ice anomalies in the Sea of Okhotsk, using AGCM simulations as well as observational data. They found that ice extent anomalies in this region excite a stationary wave train that extends along a great circle over Eastern Asia, the Bering Sea, and into North America. Based on AGCM results, Huang et al. (1995) found that winter sea ice over Barents Sea and Kara Sea can influence summer precipitation over China. The study of Song and Sun (2003) indicates that precipitation over North China is positively correlated with spring Arctic sea ice.

The precipitation over East Asia is dominated by the EASM. In fact, the EASM leads to 40–50 % (60–70 %) of the annual precipitation in the Yangtze River region (North China) (e.g., Gong and Ho 2003). The monsoon establishes along the Yangtze River valley and extends to South Korea and Japan in June and July. A large amount of rainfall occurs along the Meiyu-Changma-Baiu front (marked by the rectangle in Fig. 3a) that reflects a contrast between the polar cold and the tropical warm air masses. Although the climatological mean of the EASM is rather well understood, it still poses a challenge to the community to better understand the monsoon variability.

The mechanism how spring Arctic sea ice influences the summer climate over East Asia is not fully understood. For example, previous studies have suggested that Arctic sea ice variability affects the Eurasian snow cover which itself exhibits a multi-month climatic memory and thus may provide an anomalous heating/cooling forcing on the summer climate over East Asia (Zhao et al. 2004; Wu et al. 2009a, b). The induced surface changes in temperature and moisture lead to Rossby wave train excitation influencing the Asian summer monsoon. These studies emphasize the importance of persistent, anomalous land and atmosphere conditions in upstream regions (Eurasian continent) of East Asia. However, the EASM is also strongly influenced by atmospheric and oceanic states over the North Pacific (Chang et al. 2000a, b), which, in turn, are affected by changes in the sea ice cover (Chiang et al. 2003, 2005). The main question addressed in this study is: Does the ocean play a significant role in linking spring Arctic sea ice and EASM variability?

The main purpose of the present study is to investigate a new possible mechanism of how the spring Arctic sea ice impacting the EASM by using observational data, AGCM and AOGCM simulations. The paper is organized as follows. A description of data, model system, and model experiments are given in Section 2. The results from observational analysis and model simulations are presented in Sections 3 and 4, respectively. The paper closes with a discussion and concluding remarks in Section 5.

2 Data and models

2.1 Data and method

The data used in this study include the National Center for Environmental Prediction-National Center for Atmospheric Research reanalysis products with a horizontal resolution of 2.5°×2.5° (Kalnay et al. 1996), monthly sea ice area (SIA) data from the National Snow and Ice Data Center (Fetterer et al. 2002), monthly sea ice concentration (SIC) data from the British Atmospheric Data Centre (BADC) with a resolution of 1°×1° (http://badc.nerc.ac.uk/data/hadisst), the CPC Merged Analysis of Precipitation (CMAP) with a resolution of 2.5°×2.5° (Xie and Arkin 1997), and monthly gridded Extended Reconstructed Sea Surface Temperature (v3b) data with a resolution of 2°×2° (Smith et al. 2008). All analyses are confined to the period 1979 to 2009.

We focus on the interannual timescale variations for all climate variables in the present study. The decadal and long-timescale variabilities are removed by using a 10-year Butterworth filter to the climate variables before analysis (Butterworth 1930). The correlation method applied is Pearson correlation (Rodgers and Nicewander 1988). The significance of Pearson correlation coefficient is computed by transforming the correlation to create a t statistic with n-2 degrees of freedom, where n is the number of rows of variables. The confidence bounds are based on an asymptotic normal distribution. Furthermore, multivariate Empirical Orthogonal Function (MV-EOF) analysis (Wang 1992) is used to obtain the co-variance of East Asian summer precipitation and spring ASIC. Finally, we applied regression analysis to climate variable (Y) and El Niño Southern Oscillation (ENSO) index (X), and we assume the residual part of the climate variable (Y) is signal excluding the ENSO impact. This method has been used by early studies (e.g., Gong et al. 2011). It should be mentioned that our results are still robust if the ENSO signal is linearly removed.

2.2 Model description

The second version of Bergen Climate Model (BCM2; Otterå et al. 2009) is used in this study. The BCM (Furevik et al. 2003) was one of the contributing models to the last IPCC report (Meehl et al. 2007) and has been used in a wide range of climate studies (e.g., Bentsen et al. 2004). The BCM2 has been improved in various aspects compared with the original BCM (see Otterå et al. 2009 for details). Importantly, conservation properties of the ocean model have been largely improved by adopting an incremental remapping scheme and the single layer sea ice model has been replaced with the multi category model GELATO (Salas-Mélia 2002). The atmospheric component is the

spectral model ARPEGE/IFS (Déqué et al. 1994), which in our configuration has 30 vertical hybrid levels and a horizontal resolution of approximately 2.8°. The ocean component is based on but is a heavily modified version of the isopycnic coordinate model MICOM (Bleck and Smith 1990), which has an average horizontal resolution of approximately 2.4° with enhanced resolution in the tropics and in the Arctic and a stack of 34 isopycnic layers with a bulk-mixed layer on top (see Lohmann et al. 2009 for more details).

2.3 Experiments design

The baseline integrations for this study comprise two coupled simulations that are integrated over 120 years: one present-day control integration (PCTRL) with atmospheric CO_2 concentrations kept constant at the year 2000 level, and one future scenario integration (FCTRL) that follows the IPCC A2, business-as-usual scenario. During 101–120 years of FCTRL, the CO_2 concentration is fixed at 992 ppm. To explore how the spring ASIC anomalies impact the EASM, we performed spring ASIC perturbation experiments with BCM2 and the atmosphere-only model ARPEGE/IFS, which is the atmospheric component of BCM2. The so-called "atmospheric bridge and oceanic tunnel" (ABOT; Yang and Liu 2005) technique is implemented for the sea ice perturbation experiment performed by BCM2. The ABOT technique has been successfully applied in previous studies to address tropical-extratropical climate interactions (e.g., Su et al. 2008). Following numerical experiments have been designed to isolate the role of spring Arctic sea ice and air–sea coupling (ocean changes):

- Atmosphere-only control experiment (A-CTRL): lower boundary conditions are obtained from the daily, climatological mean of ocean–sea ice output from the first 100 years of PCTRL. Integrated for 30 years.
- Atmosphere-only sea ice perturbation experiment (A-SICE): the same as A-CTRL, but with the spring ASIC and sea surface temperature (SST) from the daily, climatological mean of the last 20 years of FCTRL when the spring ASIC in the Sea of Okhotsk and the Barents Sea is essentially zero.
- Atmosphere-only SST perturbation experiment (A-SST): same as A-CTRL, but with superposed summer SST anomalies in the North Pacific to explore the impact of North Pacific SST anomalies that are associated with anomalous spring sea ice on the EASM. Integrated for 30 years.
- ABOT-coupled control experiment (AO-CTRL): inside the Arctic region (defined by the maximum ice extent in PCTRL), spring Arctic SICs and SSTs are prescribed with daily climatological values that are obtained from the last 20 years of PCTRL. Outside the Arctic region, the system remains fully coupled. Integrated for 60 years.
- ABOT-coupled sea ice perturbation experiment (AO-SICE): same as AO-CTRL but with the spring ASICs and SSTs obtained from the last 20 years of FCTRL. Integrated for 60 years.

The difference between AO-SICE and AO-CTRL provides the spring sea ice impact on the climate in the coupled model; whereas the difference between A-SICE and A-CTRL provides the spring sea ice impact on climate in the atmosphere-only model. The difference between the A-SST and A-CTRL provides the impact of summer SST anomalies in the North Pacific, that are associated with reduced sea ice, on the climate in the atmosphere-only model.

3 Results from observations

3.1 The linkage between spring Arctic SIA and EASM

The EASM index is often used to describe the precipitation and circulation associated with the EASM. Here, we employed the Wang and Fan (1999) index and the Lau et al. (2000) index, which are based on the horizontal zonal wind shears at 850 and 200 hPa levels, respectively, emphasizing features in the lower and upper troposphere. The Wang and Fan (1999) index performs well in capturing the total variance of precipitation and circulation over East Asia (Wang et al. 2008). The EASM indices are computed using the following formulae:

Wang and Fan (1999)

$$\text{Index}: \mathrm{U850}(5^{\circ}\text{--}15^{\circ}\,\mathrm{N},\ 90^{\circ}\text{--}130^{\circ}\,\mathrm{E})\text{minus}\ \mathrm{U850}(22.5^{\circ}\text{--}32.5^{\circ}\,\mathrm{N},\ 110^{\circ}\text{--}140^{\circ}\,\mathrm{E});$$

Lau et al. (2000)

$$\text{Index}: \mathrm{U200}(40^{\circ}\text{--}50^{\circ}\,\mathrm{N},\ 110^{\circ}\text{--}150^{\circ}\,\mathrm{E})\text{minus}\ \mathrm{U200}(25^{\circ}\text{--}35^{\circ}\,\mathrm{N},\ 110^{\circ}\text{--}150^{\circ}\,\mathrm{E});$$

Where U850 and U200 denote the zonal wind at the 850 and 200 hPa, respectively.

Figure 1b shows the timeseries of February–March–April (FMA)-averaged Arctic SIA and June–July–August (JJA)-averaged Lau et al. (2000) index. The computation of lagged correlations reveals that the ice area during FMA has the strongest correlation with the monsoon index during JJA, with a correlation coefficient of $r=-0.42$ which is significant at the 95 % confidence level (Fig. 1a). The FMA Arctic

SIA correlates negatively with the monsoon index (Fig. 1b). We also computed the Arctic SIA correlation with the Wang and Fan (1999) index, yielding a significant value of −0.35. The three-dimensional structure of atmospheric circulation changes over East Asia that project onto Arctic SIA changes was further investigated. For positive spring Arctic SIA anomalies, it follows that the JJA East Asian westerly jet (at about 40° N in climatology) tends to move southward and wind shear between 40–50° N, 110–150° E, and 25–35° N, 110–150° E tends to decrease (Fig. 2a), and that an anomalous westerly wind centre appears between 20° and 30° N, extending vertically from 1,000 to 100 hPa. These anomalous westerlies are flanked by two regions of anomalous easterlies that are located south of 20° and north of 35° N and extend approximately from 700 to 150 hPa (Fig. 2b). In other words, anomalous westerlies are present in the subtropics throughout the troposphere, and anomalous easterlies are present at ~40° and ~10°N from mid- to upper tropospheric levels. These summer wind anomalies are associated with larger-than-average spring Arctic SIA, and they are present in the whole troposphere and have well-defined vertical structures: stronger downwelling at ~20° N and intensified upwelling at ~30° N, implying anomalous precipitation at these latitudes

3.2 Spring Arctic SIA and precipitation in East Asia

As shown in the previous section, related to anomalous spring Arctic SIA there are significant summer atmospheric circulation changes over East Asia. These circulation changes are expected to lead to corresponding precipitation changes, i.e., anomalous dry conditions in areas with anomalous descending motion and anomalous wet conditions in areas with anomalous ascending motion. For larger-than-average spring Arctic SIA, these areas are located south of 25° N and north of 25° N, respectively. As shown in Table 1, the spring Arctic SIA is significantly correlated with the two EASM indices and summer precipitation over East Asia. The correlations with precipitation are −0.40 and +0.35 in the southern and northern regions, respectively. Both are significant at the 95 % confidence level. This indicates that for a smaller-than-average spring Arctic SIA there tend to be a higher EASM index and more precipitation in southern region and less precipitation in northern region. The summer precipitation in these two regions has an obvious out of phase relationship with a correlation coefficient of −0.57.

The leading mode of summer precipitation over East Asia (south of 45° N) has a south–north dipole structure which is projected onto the typical three-dimensional monsoon circulation variability (Fig. 3a). Wang et al. (2008) from the MV-EOF analysis found that the leading spatial mode shows a north–south dipole pattern in precipitation with two opposite anomalous regions similar to Fig. 3a. One region is located over the northern China south sea with a west–east orientation (around 15° N) and the other region spans from the Yangtze River valley to southern Japan (around 30° N), which covers the prevailing Meiyu-Changma-Baiu front area (marked by the rectangle in Fig. 3a). Figure 3b shows the spatial distribution of the correlations between the spring Arctic SIA and the JJA precipitation in East Asia and western North Pacific. A clear dipole pattern emerges in East Asia, closely resembling the monsoon-related precipitation pattern (Gu et al. 2009). The similarity of the spatial structures suggests a potential connection between the EASM rainfall and the preceding spring Arctic SIA. The summer precipitation associated with spring Arctic SIA variability can account for ~20 % of the precipitation variability in the tropical North Pacific and 7–10 % in the subtropical (~30° N) and northern (~45° N) North Pacific.

It is generally recognized that the ENSO has a large influence on the climates over north-western Pacific and East Asia (e.g., Wang et al. 2000; Ding et al. 2011). After regressing out the ENSO signal in the climate variables (SIA and EASM), the correlation between spring Arctic SIA and the EASM index of Lau et al. (2000) is still significant (r= −0.4), and the spatial distribution of correlations between the spring Arctic SIA and the East Asia summer precipitation is nearly identical to the case where the ENSO influence is not removed. Therefore, the connection between the spring Arctic SIA and the summer precipitation over East Asia is likely independent of ENSO.

3.3 Anomalies of 850 hPa winds and 500 hPa heights over North Pacific

The western North Pacific subtropical high (WNPSH) and monsoon trough are two important components of the EASM circulation system (e.g., Tao and Chen 1987; Wu and Wang 2000). For a positive anomalous spring Arctic SIA, the most important feature of the anomalous wind at 850 hPa is a statistically significant anomalous cyclonic circulation over the south of Japan and an anomalous anticyclonic circulation over the central North Pacific extending into south China (Fig. 4a). Previous studies (e.g., Wang and Fan 1999; Wang et al. 2008) have reported that a similar cyclonic pattern over the south of Japan can be identified as the inherent mode of the EASM. This means that following a larger-than-normal spring Arctic SIA, there would be anomalous convergence of air-flow in about 30° N, implying above-than-normal precipitation along the Meiyu-Changma-Baiu belt. Anomalous upward air motion occurs in 25–35° N along 120° E, coinciding with the location of anomalous cyclonic circulation and anomalous downward air motion at approximately 10–20° and 35–45° N (Fig. 2b). The anomalous circulation patterns can explain the

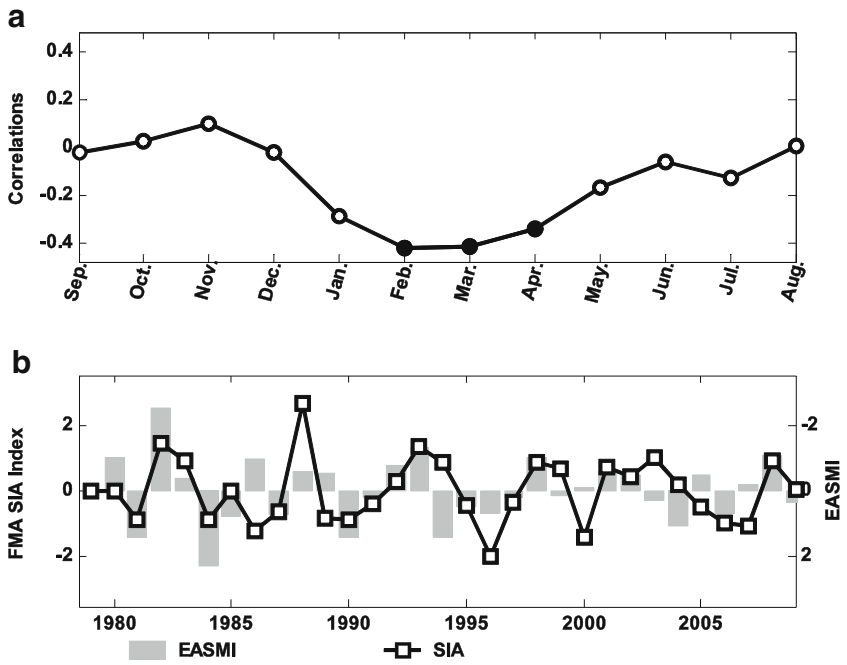

Fig. 1 **a** Correlation between monthly Arctic SIA and East Asian summer monsoon index defined by Lau et al. (2000). **b** Normalized timeseries of spring Arctic SIA and East Asian summer monsoon index. All the timeseries are 10-year high-pass filtered using a Butterworth filter. To facilitate comparison, the vertical axis for monsoon index has been reversed

enhanced summer precipitation at about 30° N and the reduced summer precipitation at 10–20° N in larger spring Arctic SIA years.

The WNPSH plays an important role in regulating the location of the rain belt and modulating moisture transportation at both interannual and decadal timescales. More precipitation tends to occur along the Yangtze River through southern Japan when the WNPSH moves southward or extends more westward. In contrast, drier conditions are favored by a northward displacement or an eastward retreat of the WNPSH (Chang et al. 2000a, b; Gong and Ho 2002). As indicated in Fig. 4a, for larger-than-normal spring Arctic SIA, there is an anomalous Z500 minimum to the south of Japan extending to the Bering Sea, and an anomalous maximum in the subtropical central North Pacific extending to the south of China, both of which are statistically significant. This west–east oriented dipole pattern suggests an eastward retreat of the WNPSH. To illustrate the temporal variations of WNPSH, we defined the regional average 500-hPa heights over 15–35° N and 150–180° E as the WNPSH index. The time series of the summer WNPSH index and the spring Arctic SIA are significantly correlated with a correlation coefficient of r=+0.45 for the period 1979–2009 (Fig. 4b). It is well known, that the WNPSH is strongly modulated by the ENSO signals. When we remove the ENSO signals, the correlation between WNPSH and the spring ASIA is still statistically significant with a correlation coefficient of +0.30. This implies that the connection between spring Arctic SIA and WNPSH is very likely independent of ENSO.

3.4 Persistent large-scale circulation anomalies over North Pacific

Our observational analysis has demonstrated the existence of robust and consistent co-changes in monsoon indices, atmospheric circulations, and regional precipitation in summer that

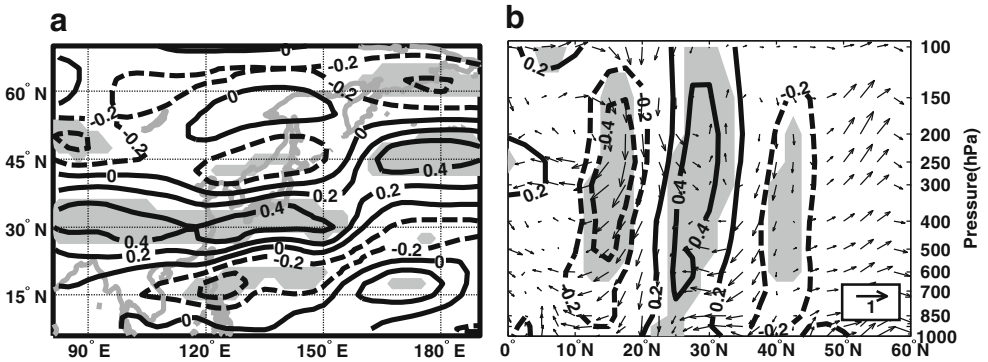

Fig. 2 **a** Correlation coefficients between the spring Arctic SIA and the summer 200-hPa zonal wind. **b** The JJA correlation coefficients of zonal (u), meridional (v), and vertical (w) winds in association with the spring Arctic SIA along 120° E. The w and v are shown as vectors and u as contours with intervals of 0.2. *Shadings* indicate that the correlation coefficients exceed the 0.05 confidence level

Table 1 Correlation coefficients between FMA Arctic SIA and EASM indexes and the regional precipitation for the period 1979–2009

	Lau et al. (2000) index, JJA	Wang and Fan (1999) index, JJA	South precipitation, JJA	North precipitation, JJA
FMA SIA	−0.42[a]	−0.35[a]	−0.40[a]	+0.35[a]
JJA South precipitation[c]	+0.66[b]	+0.76[b]	–	−0.57[b]
JJA North precipitation[d]	−0.52[b]	−0.62[b]	−0.57[b]	–

[a] Significant at the 95 % level

[b] At the 99 % level

[c] Mean precipitation averaged over southern region over 10–25° N, 110–150° E

[d] Mean precipitation averaged over northern region over 25–35° N, 110–150° E

are associated with the preceding spring Arctic sea ice anomalies. In the following, we examine more details of the atmospheric circulation and SST changes from spring to summer to shed light on the possible mechanism(s) how spring Arctic sea ice variations impact the EASM climate.

Since SIC instead of SIA can provide both spatial and temporal variations, we performed MV-EOF analysis on the East Asian summer precipitation and spring ASIC in order to extract their co-variances. The spatial pattern of the leading MV-EOF mode of the East Asian summer precipitation (Fig. 5a) is general consistent with the spatial pattern of EASM-associated precipitation showing two regions with opposite anomalous precipitation (Fig. 3a).

For the Arctic sector, it is obvious that the variations of spring ASIC were not uniform in space and time over the past 30 years (Fig. 5b, c). The spring ASIC have generally increased in the Bering Sea and Davis Strait while they have decreased in the Sea of Okhotsk and the Barents Sea. The leading MV-EOF modes account for about 15 % of the covariance.

Since we focus on the interannual timescale, in the following, we correlate the 10-year high-pass filtered first principal component (PC1) (Fig. 5c) with the SST in North Pacific from spring (March–April–May) to JJA.

The main feature of anomalous SST evolution related with PC1 is a dipole SST pattern with negative and positive SST anomalies in the western tropical and subtropical north Pacific persisting from spring to summer (Fig. 6a–d). The SST dipole is statistically significant at 95 % level. One pole is centred around 25–35° N along 150° E, and the other pole spans almost the entire western tropical North Pacific with the centre around east of Philippines. Associated with the dipole SST anomalies, there are well defined and steady atmospheric circulation anomalies from spring to summer. The main circulation features at 850 hPa are an anomalous anticyclone covering the tropical and subtropical North Pacific (0–40° N), and an anomalous cyclone centered over the Bering Sea from late spring (April–May–June) to summer. The anomalous anticyclonic 850 hPa circulation from spring through summer implies Ekman transport convergence of surface water (Gong et al. 2011) and therefore leads to positive SST (25–35° N, 150° E). The anomaly pattern of the 500-hPa height response (Fig. 7a–d) is similar to the anomaly pattern of 200 hPa streamlines (not shown), supporting an equivalent barotropic structure of the anomalous large-scale circulation.

It should be emphasized here that the 850 hPa wind anomalies become statistically significant in late spring and strengthen in early summer (MJJ) in the tropics and subtropics. An anomalous high pressure over the central North Pacific and an anomalous low pressure covering the high latitudes over the North Pacific indicate an intensified and more westward extended WNPSH, implying a strengthened south-easterly wind from the Pacific Ocean and more moisture from West Pacific and potentially increased precipitation over Meiyu-Changma-Baiu belt (Zhou and Yu 2005). The persistent atmospheric circulation and SST

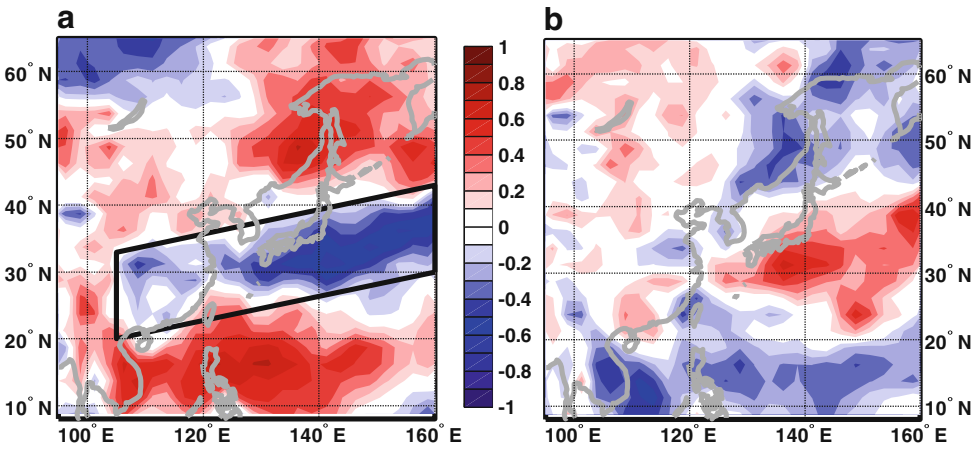

Fig. 3 **a** The correlations between the precipitation and EASM index of Lau et al. (2000). **b** Correlations between the precipitation and the spring Arctic SIA. All correlation was computed after being 10-year high-pass filtered

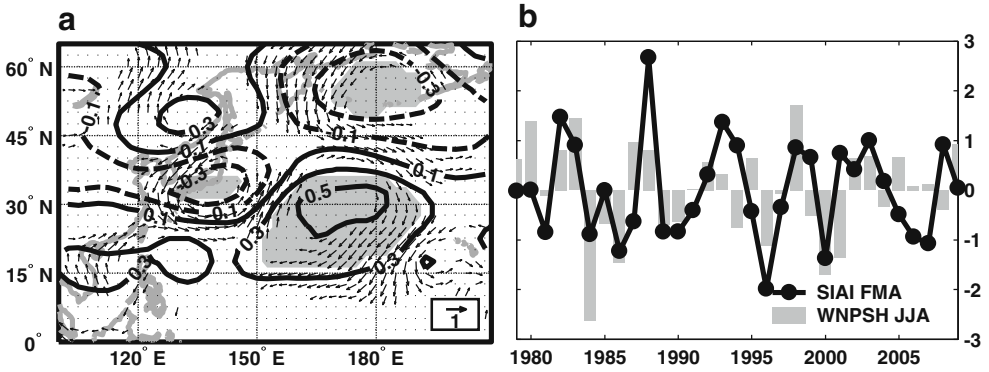

Fig. 4 **a** Correlation coefficients between spring Arctic SIA and summer 500-hPa geopotential heights (*solid/dashed contour lines* denote positive/negative correlation. *Shading* indicates significant at the 95 % level). The vectors denote the significant (95 % level) correlation coefficients between summer 850-hPa wind and spring Arctic SIA. **b** Timeseries of the normalized spring Arctic SIA and the intensity of the summer WNPSH, which is defined as the regional mean 500-hPa heights averaging over 15–35° N and 150–180° E

anomalies over the North Pacific provide a possible mechanism on how the spring sea ice anomalies impacting the EASM. To summarize our observational-based analysis, we can propose the following mechanism (Fig. 8) on how the spring Arctic sea ice impacting the EASM: spring Arctic sea ice anomalies cause atmospheric circulation anomalies, which, in turn, cause SST anomalies in the North Pacific. The SST anomalies can persist into summer and then impact the summer monsoon circulation and precipitation over East Asia.

4 Results from numerical simulations

Before we discuss the climate impact of spring sea ice, we evaluate the simulated climatology of summer precipitation

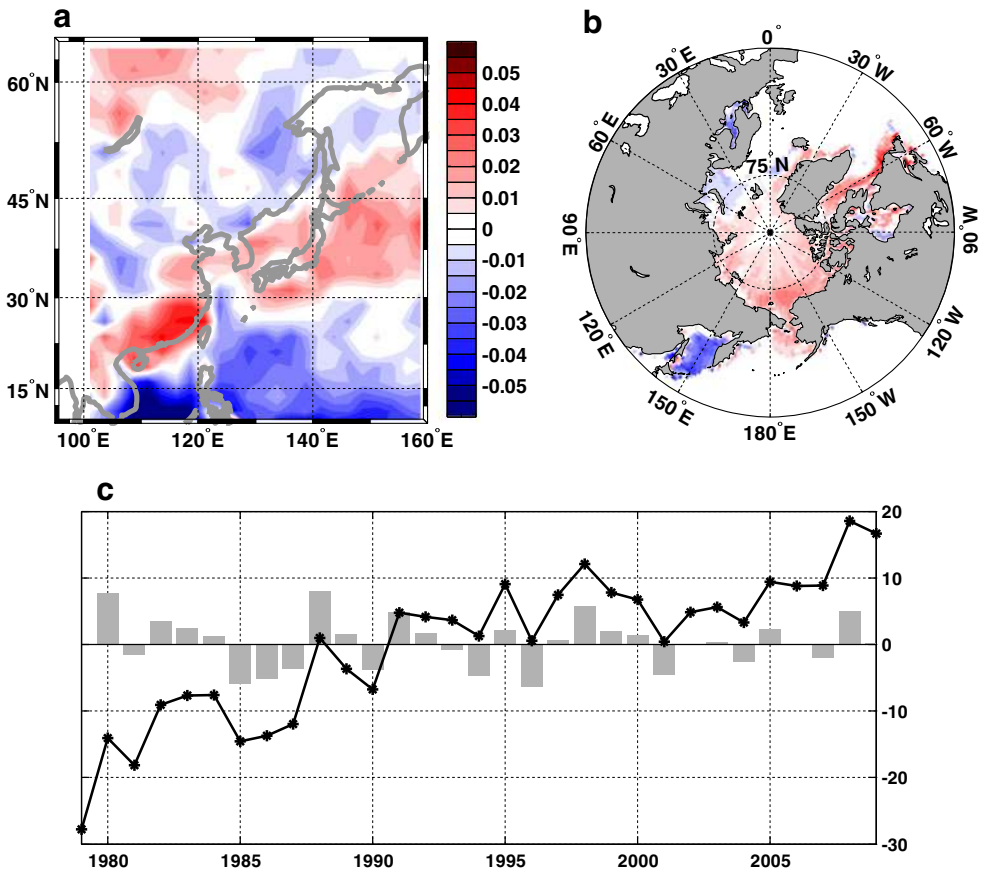

Fig. 5 The spatial pattern of the leading MV-EOF mode of **a** normalized East Asian summer precipitation and **b** normalized spring Arctic sea ice concentration. **c** First component (PC1) of the leading MV-EOF modes (*solid line*). The *bars* denote the PC1 after being 10-year high-pass filtered

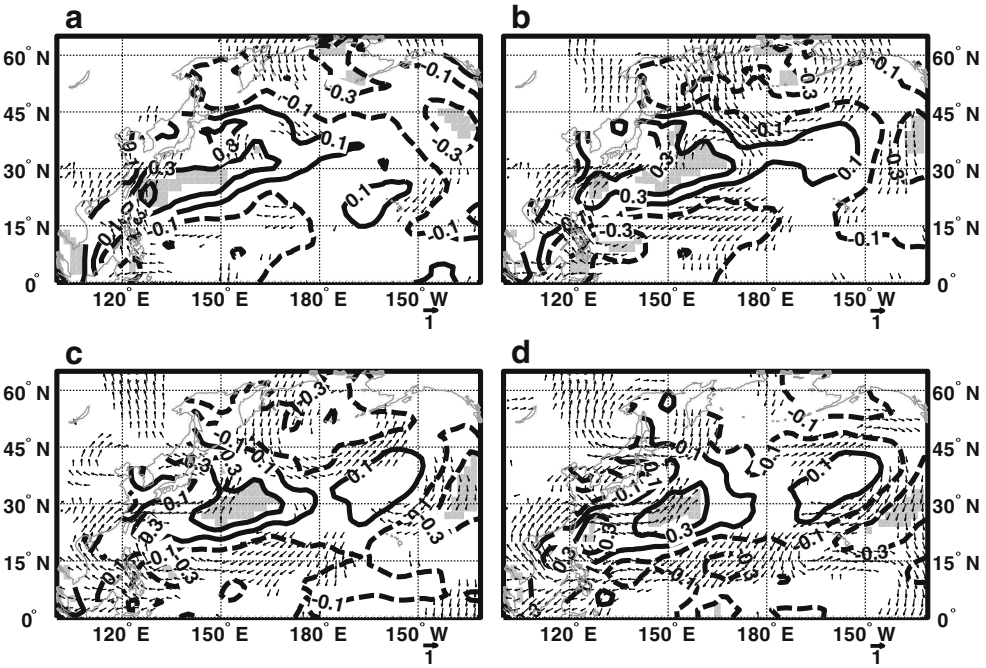

Fig. 6 Correlation between leading MV-EOF PC1 (10-year high-pass filtered) and SSTs (*solid/dashed contour lines* denote positive/negative correlations. *Shadings* indicate significant at the 95 % level). The vectors denote the significant (95 % level) correlation coefficients between 850-hPa wind and leading MV-EOF PC1. In all figures, leading MV-EOF PC1 is confined to spring Arctic sea ice concentration while SSTs and winds are for MAM (**a**), AMJ (**b**), MJJ (**c**), and JJA (**d**)

over East Asia. The simulated precipitation in AO-CTRL (Fig. 9b) qualitatively matches the observations (Fig. 9a) with polarward and eastward decrease pattern (start from 120° E). Particularly, the observed spatial distribution of the precipitation east to 110° E is well reproduced. However, the precipitation in the Intertropical Convergence Zone of North Pacific is underestimated by 2 mm/day (figure not shown). The simulated change in East Asian summer precipitation caused by the reduced spring sea ice (AO-SICE minus AO-CTRL) (Fig. 9d), with a negative along Meiyu-Changma-Baiu region (around 30° E) and a positive response over the South China Sea and the Philippines, reproduces the observed zonal dipole pattern (south of 45° N) that is associated with smaller-than-normal spring Arctic SIA (Fig. 3b). This implies that our coupled experiments have the capacity to represent the climate impact of reduced spring ASIC on East Asia. The atmospheric circulation anomalies at 850 hPa (Fig. 10b) caused by the reduction of spring Arctic sea ice qualitatively matches the circulation anomalies derived from the observation-based analysis

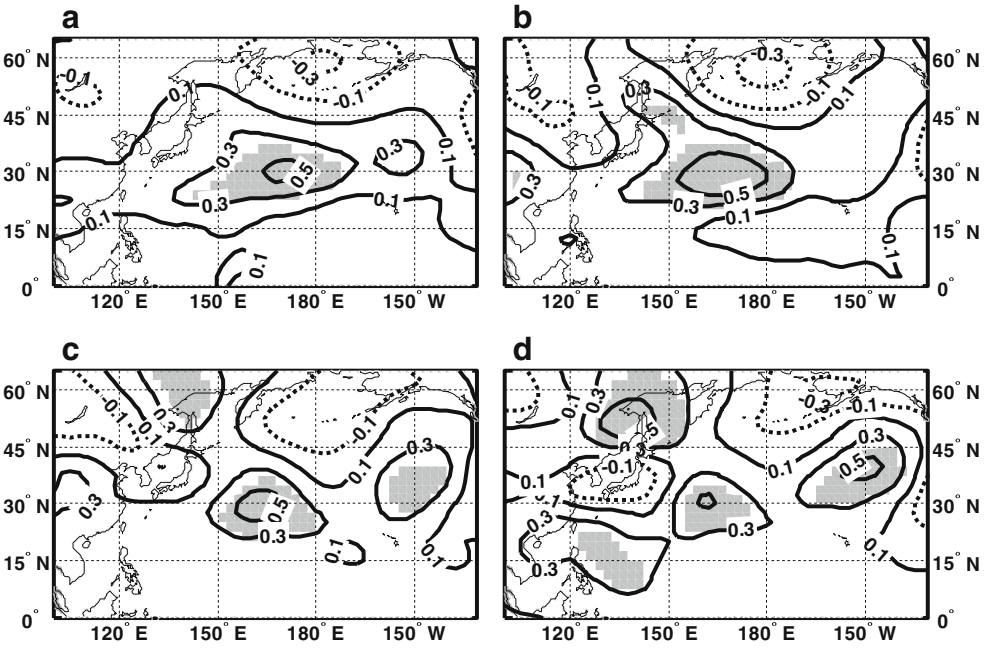

Fig. 7 Correlation between the leading MV-EOF PC1 (10-year high-pass filtered) and 500-hPa geopotential height (*solid/dashed contour lines* denote positive/negative correlations. *Shadings* denote significant at the 95 % level) for MAM (**a**), AMJ (**b**), MJJ (**c**), and JJA (**d**)

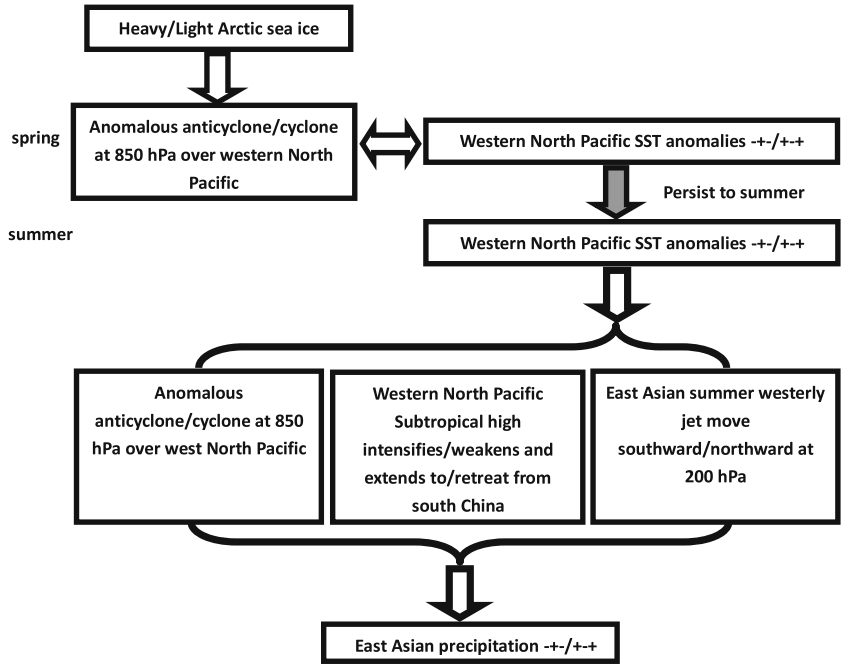

Fig. 8 Schematic summary of the proposed mechanism

(Fig. 4a). Also the anomalous cyclone that is simulated over the western tropical North Pacific is in good agreement with the observation-based analysis. The simulated summer response in low-level winds to reduced Arctic spring sea ice is

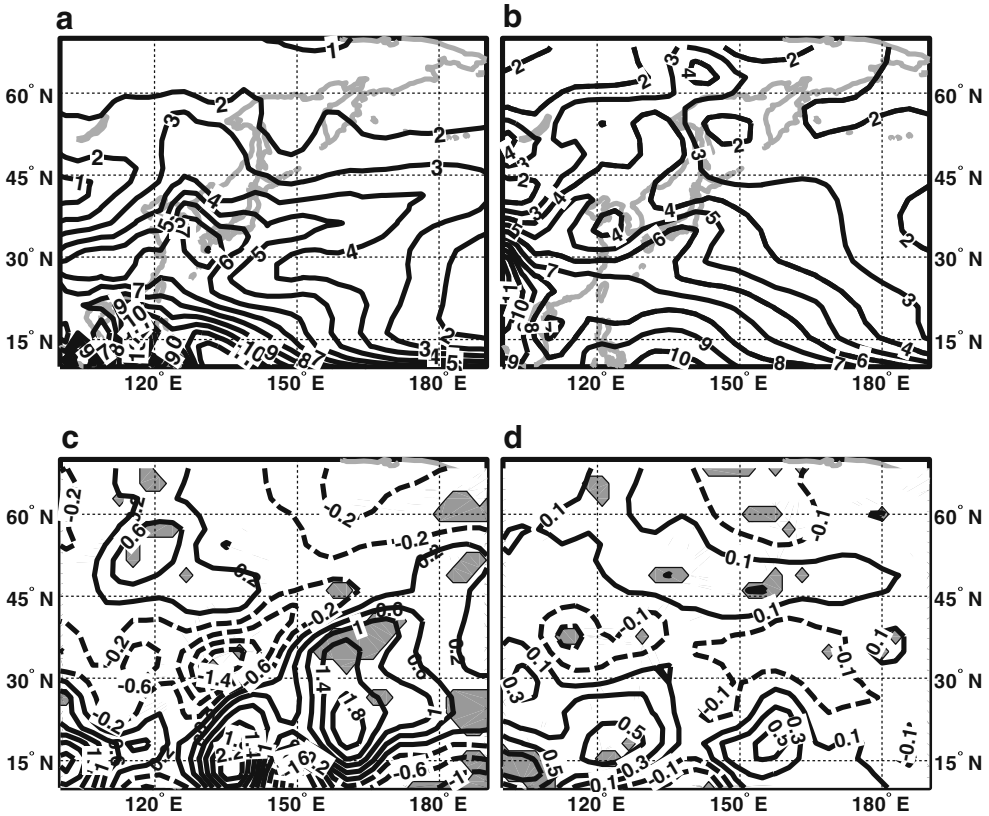

Fig. 9 The observed (**a**) and simulated (**b**) summer precipitation (in millimeters per day; observation/simulation is from CMAP/PCTRL, respectively). Difference in summer precipitation (in millimeters per day) caused by **c** SST impact (A-SST minus A-CTRL) and **d** reduction in spring Arctic sea ice (AO-SICE minus AO-CTRL)

an anomalous eastward flow that spans from the North Pacific to the Yangtze river basin along 30° N, then becomes a southward flow along 110° E, and finally a westward flow at ~10° N. This wind anomaly pattern could explain why the simulated west–east orientated precipitation belt is opposite to the one in the observational analysis, and that the anomalous anticyclone (cyclone), which centered over Japan in the observations (Fig. 4a), is shifted eastward to the North Pacific for light sea ice condition in our simulation (Fig. 10b) relative to the observational analysis. Correspondingly, the anomalous precipitation belt is not centered over south Japan as it is the case in the observation.

For the mid- and upper troposphere, the WNPSH and the East Asian westerly jet stream are two major large-scale circulation systems that dominate the EASM. As shown in Fig. 11a, main patterns of 500 hPa geopotential height anomalies is consistent with Figs. 4a and 7d. In our simulations for the negative spring sea ice case, there is an anomalous minimum along 30° N centred around 180° E, which is adjacent to an anomalous maximum over the southeast of Japan, indicating a slight northward shift of WNPSH. This pattern is also consistent with the anomalous wind at 850 hPa (Fig. 10) and anomalous precipitation pattern (Figs. 3 and 9d).

Previous studies indicated that the north–south shifting of the jet plays an important role for the monsoon onset and retreat and hence for anomalous monsoon rainfall (Liang and Wang 1998; Gong and Ho 2003). Furthermore, the location of the Meiyu fronts that produce an extensive summer monsoon rainfall is highly related to the location of the westerly jet stream. Thus, the jet stream can be used as a representative circulation for the summer monsoon. The coupled spring sea ice sensitive simulations can also capture these features shown in Fig. 11b. The simulated pattern is similar to the one obtained from the observational correlation analysis (Fig. 2a) but has the opposite sign because the simulation results reflect the response to reduced spring Arctic sea ice. This implies a south–north movement of the middle latitude zonal jet over East Asia in our simulations for the less spring sea ice case. However, the A-SICE experiment (figure not shown) cannot capture this anomalous zonal wind pattern at 200 hPa in summer. This indicates that the role of the air–sea coupling in linking spring Arctic sea ice and the summer zonal wind jet at 200 hPa. The results of AO-SICE further confirm the summer East Asia westerly jet at 200 hPa in summer (weakened around 30° N and strengthened around 45° N following the reduced spring Arctic SIA, Fig. 11b).

The definition of the strength of the EASM employed in this study is the difference in 200 hPa zonal wind between averaged values over the domains 40–50° N, 110–150° E and 25–35° N, 110–150° E (Lau et al. 2000), meaning that the East Asian jet plays an essential role in the dynamical

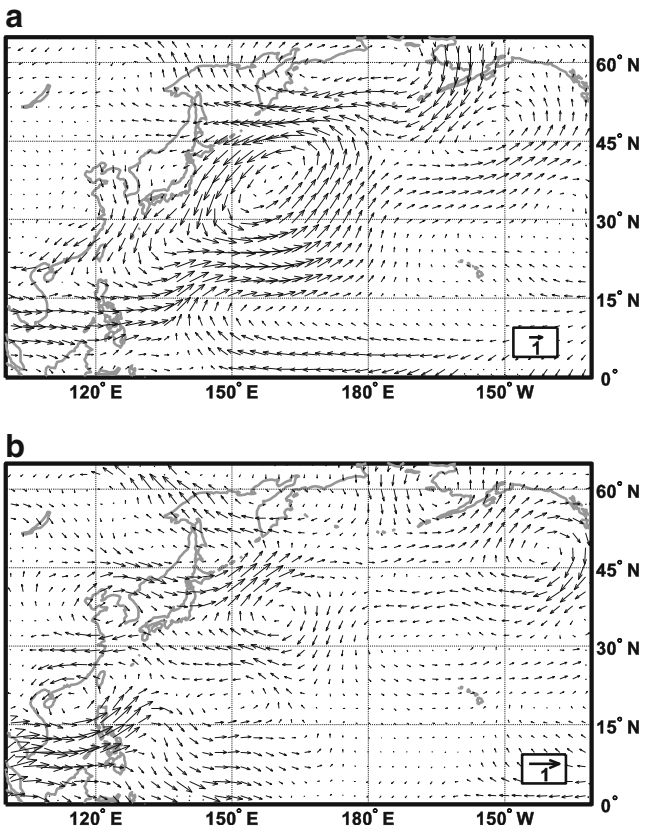

Fig. 10 Difference (in meters per second) in summer 850-hPa atmosphere circulation caused by **a** SST anomalies (A-SST minus A-CTRL) and **b** reduction of spring Arctic sea ice (AO-SICE minus AO-CTRL)

aspect of the summer monsoon. The aforementioned pattern associated with the negative phase of spring sea ice generally resembles the strong EASM years (Lau et al. 2000). This simulated northward shifting of the westerly jet stream accompanies the pattern of anomalous precipitation, producing less precipitation over the Meiyu belt as response to reduced spring Arctic sea ice (Fig. 9d). These atmospheric circulation features are all consistent with that in precipitation and further confirm the existence of a sea ice-monsoon rainfall connection.

As indicated by the observation-based analysis, SST is potentially an important factor for bridging the spring sea ice and the EASM-induced precipitation. Figure 12 shows the SST anomalies that are simulated as the response to reduced spring Arctic SIA (AO-SICE minus AO-CTRL). The anomalous spring SST pattern (Fig. 12a) is generally consistent with the result of observation-based analysis (Fig. 6a) for the low-mid-latitudes, but the anomaly signal is opposite over the east of Japan. Nevertheless, for the remaining part of the North Pacific, the anomalies are consistent with the result from observation-based analysis. The main structure comprises a belt of the anomalously high SST that spans from the sea of Philippines to Mexican Bay along the tropical North Pacific. Anomalous low SST

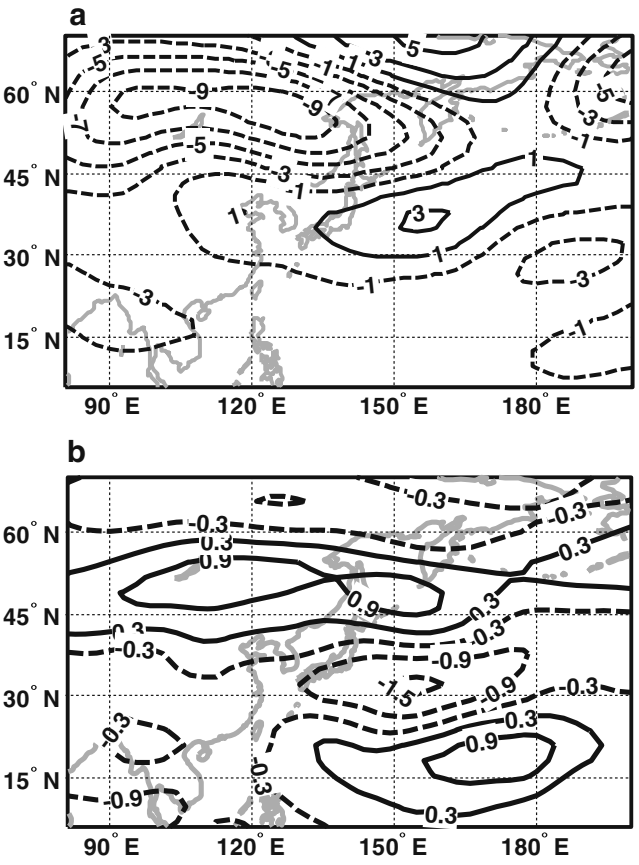

Fig. 11 **a** Difference in summer (JJA) geopotential height (in meters) at 500 hPa between the AO-SICE and AO-CTRL and **b** difference in summer (JJA) zonal wind (in meters per second) at 200 hPa between the AO-SICE and AO-CTRL

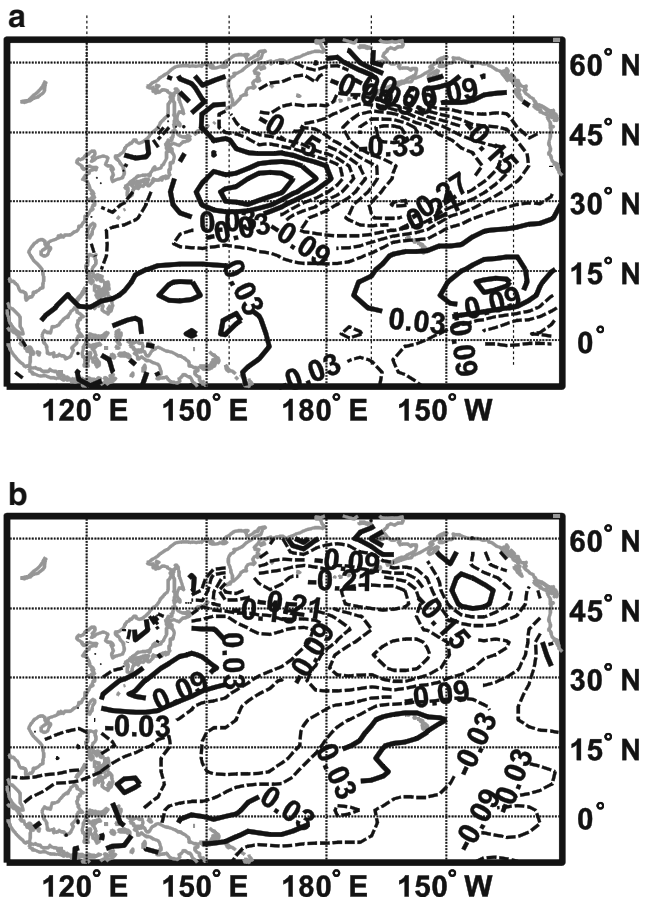

Fig. 12 The SST difference (in degrees Celsius) caused by the reduction of spring Arctic sea ice (AO-SICE minus AO-CTRL) for **a** spring and **b** summer

is simulated around the mid-latitude of the North Pacific. This dipole of SST anomalies (except over the east Japan) is consistent with the result from the observation-based analysis and persists from spring (Fig. 12a) to summer (Fig. 12b). This is also why our model can capture the spatial response pattern of precipitation.

Furthermore, the spatial distribution of the anomalous precipitation (A-SST minus A-CTRL) from the AGCM-only with the SST anomalies exactly resembling the pattern in Fig. 6c shows a northeast tilted triple pattern (Fig. 9c) compared with the zonal triple pattern in the observations (Fig. 3b). The results confirm that the summer SST anomalies in the North Pacific associated with the MV-EOF PC1 of the spring ASIC can lead to atmospheric circulation anomalies (Fig. 10a) which are consistent with the statistical analysis (Fig. 6d) and by that to the East Asian summer (JJA) precipitation anomalies.

It should be mentioned that the climate impact of the reduced spring Arctic SIA simulated by AGCM-only (A-SICE minus A-CTRL) cannot reproduce the observed dipole pattern of summer precipitation anomalies (figure not shown here), implying the evolution of North Pacific SST being the linkage between the spring Arctic sea ice and the EASM precipitation.

5 Discussion and conclusions

Observational analysis and numerical experiments with a coupled atmosphere–ocean and an uncoupled atmosphere-only model are performed to investigate the relationship between the spring Arctic sea ice and the EASM-induced precipitation. The results from the observations and the model experiments show that the reduced spring Arctic sea ice leads to an enhancement of summer rainfall in northeast China and in the belt including the Indochinese Peninsula, South China Sea, Philippines, and the region east of Guam. Concurrently, the rainfall over Meiyu-Changma-Baiu front significantly decreases. The underlying large-scale atmospheric circulation response supports this spring sea ice–summer monsoon relationship. The reduction of the spring Arctic sea ice can lead to a dipole low-level wind response over the North Pacific, with an anomalous cyclone and an anomalous anticyclone, which, in turn, generates North

Pacific SST anomalies during spring. The spring time SST anomalies in the North Pacific can persist into summer and therefore impact the EASM precipitation. Our modelling results show that only the coupled climate model can capture the linkage of the spring Arctic sea ice and the EASM precipitation in the observation, implying the important role of air–sea interaction in bridging the spring Arctic sea ice and the EASM precipitation.

In association with larger/smaller spring Arctic SIA, the East Asian westerly jet tends to weaken/strengthen the horizontal wind shear. It seems to be directly related to the positive/negative geopotential height at about 30° N which appears in spring and persists into JJA with a little southward/northward shift (being in about 15–30° N in JJA, see Fig. 7). These barotropical height anomalies lead to anomalous eastern/western winds to the southern side and anomalous western/eastern winds to the northern side. Thus there are stronger/weaker westerlies in about 30° N in JJA (Fig. 2a). The reason(s) why there are persistent geopotential height anomalies over the northwestern Pacific, however, are not well understood. There are some possible causes: (1) the south–north thermal gradients may one reason as suggested by Francis and Vavrus (2012), (2) the diabatic heating (such as precipitation latent heating over the northwestern Pacific between 25–40° N, see Fig. 3b), or the SST heating (Fig. 6), (3) dynamical process through teleconnection such as stationary Rossby waves. Our study has not proven the relative role of each possible cause may play and that further investigation is necessary to clarify these issues.

Previous studies also suggested that the North Pacific SST anomalies can be a bridge between the spring Arctic Oscillation and EASM precipitation (Gong et al. 2011). Using an atmosphere-land model, Zhao et al. (2004) found that the snow anomalies in the Eurasian continent caused by the spring sea ice anomalies in the Sea of Okhotsk can be a linkage for sea ice anomalies impacting the EASM precipitation. However, our simulations do not suggest major changes in the Eurasian snow cover as response to reduced spring Arctic sea ice.In our model, the air–sea interactions with the anomalous SST over the North Pacific constitute the main "bridge" for this inter-seasonal connection. How does the Eurasian continent snow cover covary with Arctic sea ice and EASM, and what are the relative and combined effects of snow cover and North Pacific SSTs in the conjunction of sea ice-EASM linkage, need further investigation with numerical experiments and observational data analysis.

In this paper, we have not carefully investigated the details of the dynamical processes by which the reduction of the spring sea ice can lead to specific atmospheric circulation anomalies in spring, but previous studies have shown that atmospheric circulation anomalies related to the Arctic Oscillation, which are similar to the ones in our simulations, can lead to anomalous SSTs in the North Pacific region (Gong et al. 2011). It should also be mentioned that we removed the spring Arctic sea ice in both the Barents Sea and the Sea of Okhotsk, and therefore, we cannot conclude if the simulated climate impact is dominated by either the Barents Sea or the Sea of Okhotsk. Further studies are necessary to clarify this question.

Acknowledgments This work was supported by Chinese National Basic Research Program (2009CB421406) and Chinese Academy of Sciences Innovation Program (XDA05110203) and by the Norwegian Research Council through the Impact of "Blue Arctic" on Climate at High Latitudes (BlueArc 207650/E10) and Exploring Decadal to Century Scale Variability and Changes in the East Asia (DecCen 193690) and the Arctic and sub-Arctic climate system and ecological response to the early twentieth century warming (ARCWARM 178239/E10) projects. Dr. Gong D.Y. was supported by the National Natural Science Foundation of China.

References

Bekryaev RV, Polyakov IV, Alexeev VA (2010) Role of polar amplification in long-term surface air temperature variations and modern Arctic warming. J Clim 23:3888–3906

Bentsen M, Drange H, Furevik T, Zhou T (2004) Simulated variability of the Atlantic meridional overturning circulation. Clim Dyn 22:701–720

Bleck R, Smith LT (1990) A wind-driven isopycnic coordinate model of the North and Equatorial Atlantic Ocean. 1. Model development and supporting experiments. J Geophys Res 95:3273–3285

Budikova D (2009) Role of Arctic sea ice in global atmospheric circulation: a review. Glob Planet Chang 68(3):149–163

Butterworth S (1930) On the theory of filter amplifiers. Experimental Wireless and the Wireless Engineer 7:536–541

Chang CP, Zhang Y, Li T (2000a) Interannual and Interdecadal variations of the East Asian summer monsoon and tropical Pacific SSTs. Part 1: role of the subtropical ridge. J Clim 13:4310–4325

Chang CP, Zhang Y, Li T (2000b) Interannual and Interdecadal variations of the East Asian summer monsoon and tropical Pacific SSTs. Part 2: Southeast China rainfall and meridional structure. J Clim 13:4326–4340

Chiang JCH, Biasutti M, Battisti DS (2003) Sensitivity of the Atlantic Intertropical Convergence Zone to Last Glacial Maximum boundary conditions. Paleoceanography 18(4):1094. doi:10.1029/2003PA000916

Chiang JCH, Bitz CM (2005) Influence of high latitude ice cover on the marine Intertropical Convergence Zone. Clim Dyn 25:477–496. doi:10.1007/s00382-005-0040-5

Déqué M, Dreveton C, Braun A, Cariolle D (1994) The ARPEGE/IFS atmosphere model: a contribution to the French community climate modeling. Clim Dyn 10:249–266

Deser C, Magnusdottir G, Saravanan R, Phillips A (2004) The effects of north Atlantic SST and sea ice anomalies on the winter circulation in CCM3. Part II: direct and indirect components of the response. J Clim 17:877–889

Ding QH, Wang B, Wallace JM, Branstator G (2011) Tropical–extratropical teleconnections in boreal summer: observed interannual variability. J Clim 24:1878–1896. doi:10.1175/2011JCLI3621.1

Fan K (2007) Sea ice cover over North Pacific, a predictor for the typhoon frequency over west North Pacific? Sci China Earth Sci 50:1251–1257

Fetterer F, Knowles K, Meier W, Savoie M (2002) Updated 2009: Sea Ice Index. National Snow and Ice Data Center, Boulder, CO

Francis JA, Vavrus SJ (2012) Evidence linking Arctic amplification to extreme weather in mid-latitudes. Geophys Res Lett 39:L06801. doi:10.1029/2012GL051000

Furevik T, Bentsen M, Drange H, Kindem IKT, Kvamstø NG, Sorteberg A (2003) Description and validation of the Bergen Climate Model: ARPEGE coupled with MICOM. Clim Dyn 21:27–51

Gong DY, Ho CH (2002) Shift in the summer rainfall over Yangtze River valley in the late 1970s. Geophys Res Lett 29(10):1436. doi:10.1029/2001GL014523

Gong DY, Ho CH (2003) Arctic Oscillation signals in East Asian summer monsoon. J Geophys Res 108(D2):4066. doi:10.1029/2002JD002193

Gong DY, Yang J, Kim SJ, Gao YQ, Guo D, Zhou TJ, Hu M (2011) Spring Arctic Oscillation-East Asian summer monsoon connection through circulation changes over the western North Pacific. Clim Dyn 37:2199–2216. doi:10.1007/s00382-011-1041-1

Gu, W., Li, C.Y., Li, W.J., Zhou, W., Chan, J.C.L. (2009) Inter-decadal unstationary relationship between NAO and east China's summer precipitation patterns. Geophys Res Lett 36:L13702. doi:10.1029/2009GL038843

Honda M, Yamazaki K, Tachibana Y (1996) Influence of Okhotsk sea-ice extent to atmospheric circulation. Geophys Res Lett 23:3595–3598

Honda M, Yamazaki K, Nakamura H, Takeuchi K (1999) Dynamic and thermodynamic characteristics of atmospheric response to anomalous sea-ice extent in the Sea of Okhotsk. J Clim 12:3347–3358

Huang SS, Yang XQ, Jiang QR, Tang MM, Wang ZM, Xie Q, Zhu YC (1995) The effects of the polar sea ice on climate (in Chinese). Journal of the Meteorological Sciences 15(4):46–56

Johannessen OM (2008) Decreasing Arctic sea ice mirrors increasing CO_2 on Decadal Time Scale. Atmospheric and Oceanic Science Letters 1(1):51–56

Johannessen OM, Bengtsson L, Miles MW, Kuzmina SI, Semenov VA, Alekseev GV, Nagurnyi AP, Zakharov VF, Bobylev LP, Pettersson LH, Hasselmann K, Cattle HP (2004) Arctic climate change: observed and modeled temperature and sea ice variability. Tellus 56A:328–341

Kalnay E, Kanamitsu M, Kistler R, Collins W, Deaven D, Gandin L, Iredell M, Saha S, White G, Woollen J (1996) The NCEP/NCAR 40-year reanalysis project. Bull Am Meteorol Soc 77:437–431

Lau KM, Kim KM, Yang S (2000) Dynamical and Boundary forcing characteristics of regional components of the Asian summer monsoon. J Clim 13(14):2461–2482

Liang XZ, Wang WC (1998) Association between China monsoon rainfall and tropospheric jets. Q J R Meteorol Soc 124:2597–2623

Lohmann K, Drange H, Bentsen M (2009) Response of the north Atlantic subpolar gyre to persistent north Atlantic oscillation like forcing. Clim Dyn 32:273–285

Magnusdottir G, Deser C, Saravanan R (2004) The effects of north Atlantic SST and sea ice anomalies on the winter circulation in CCM3. Part I: main features and storm track characteristics of the response. J Clim 17:857–875

Meehl GA et al. (2007) Global climate projections. In: Solomon S, Qin D, Manning M, Chen Z, Marquis M, Averyt KB, Tignor M, Miller HL (eds) Climate change 2007: the physical science basis. Contribution of Working Group I to the Fourth Assessment Report of the Intergovernmental Panel on Climate Change. Cambridge University Press, Cambridge

Mesquita DSM, Hodges KI, Atkinson DE, Bader J (2010) Sea-ice anomalies in the Sea of Okhotsk and the relationship with storm tracks in the Northern Hemisphere during winter. Tellus 63(2):312–323

Otterå OH, Bentsen M, Bethke I, Kvamstø NG (2009) Simulated pre-industrial climate in Bergen Climate Model (version 2): model description and large-scale circulation features. Geoscientific Model Development 2:197–212

Rodgers JL, Nicewander WA (1988) Thirteen ways to look at the correlation coefficient. Am Stat 42(1):59–66

Salas-Mélia D (2002) A global coupled sea ice–ocean model. Ocean Model 4(2):137–172

Screen JA, Simmonds I (2010) The central role of diminishing sea ice in recent Arctic temperature amplification. Nature 464:1334–1337

Smith TM, Reynolds RW, Peterson TC, Lawrimore J (2008) Improvements to NOAA's historical merged land-ocean surface temperature analysis (1880–2006). J Clim 21:2283–2293

Song H, Sun Z (2003) Spatial and temporal distributions of serious summer flood and drought in North China and their relationship to the North Arctic Sea-Ice (in Chinese). Journal of Nanjing Institute of Meteorology 26(3):289–295

Su JZ, Wang HJ, Yang HJ, Drange H, Gao YQ, Bentsen M (2008) Role of the atmospheric and oceanic circulation in the Tropical Pacific SST changes. J Clim 21:2019–2034

Tao SY, Chen LX (1987) A review of recent research on the East Asia summer monsoon in China. In: Chang CP, Krishnamurti TN (eds) Monsoon meteorology. Oxford University Press, Oxford, pp. 60–92

Wang B (1992) The vertical structure and development of the ENSO anomaly mode during 1979–1989. J Atmos Sci 49(8):698–712

Wang B, Fan Z (1999) Choice of South Asian summer monsoon indices. Bull Am Meteorol Soc 80:629–638

Wang B, Wu R, Fu X (2000) Pacific-East Asian teleconnection: how does ENSO affect East Asian climate? J Clim 13:1517–1536

Wang B, Wu Z, Li J, Liu J, Chang CP, Ding Y, Wu G (2008) How to measure the strength of the East Asian summer monsoon? J Clim 21:4449–4464

Wu BY, Zhang RH, Wang B, D'Arrigo R (2009a) On the association between spring Arctic sea ice concentration and Chinese summer rainfall. Geophys Res Lett 36:L09501. doi:10.1029/2009GL037299

Wu BY, Yang K, Zhang RH (2009b) Eurasian snow cover variability and its association with summer rainfall in China. Adv Atmos Sci 26(1):31–44

Wu RG, Wang B (2000) Interannual variability of summer monsoon onset over the Western North Pacific and the underlying processes. J Clim 13:2483–2510

Xie P, Arkin PA (1997) Global precipitation: a 17-year monthly analysis based on gauge observations, satellite estimates, and numerical model outputs Bull. Amer Meteor Soc 78:2539–2558

Yang H, Liu Z (2005) Tropical–extratropical climate interaction as revealed in idealized coupled climate model experiments. Clim Dyn 24:863–879

Zhang JT, Rothrock D, Steele M (2000) Recent changes in Arctic sea ice: the interplay between ice dynamics and thermodynamics. J Clim 13:3099–3314

Zhao P, Zhang X, Zhou X, Ikeda M, Yin Y (2004) The sea ice extent anomaly in the North Pacific and its impact on the East Asian summer monsoon rainfall. J Clim 17:3434–344

Zhou TJ, Yu RC (2005) Atmospheric water vapor transport associated with typical anomalous summer rainfall patterns in China. J Geophys Res 110:D08104. doi:10.1029/2004JD005413